Impact of structural perturbation of aluminum hydroxides by tannate on arsenate adsorption

TITLE:

Impact of Structural Perturbation of Aluminum Hydroxides by Tannate on Arsenate Adsorption

AUTHORS:

M. Martin[1,2], G. Yu[1,3], E. Barberis[2], A. Violante[4], L.M Kozak[1] and P.M. Huang[1*]

AFFILIATION:

[1] Department of Soil Science, University of Saskatchewan, 51 Campus Drive, Saskatoon, SK Canada S7N 5A8

[2] Università di Torino, DI.VA.P.R.A. – Chimica Agraria, Via L. da Vinci 44, 10095 Grugliasco (TO), Italy.

[3] Institute of Soil Science, Chinese Academy of Sciences, 210008 Nanjing, China

[4] Università di Napoli Federico II, Dipartimento di Scienze del suolo, della pianta, dell'ambiente e delle produzioni animali, Via Università, 100 - 80055, Portici (NA), Italy

CORRESPONDING AUTHOR:

*P.M. Huang, Department of Soil Science, University of Saskatchewan, 51 Campus Drive, Saskatoon, SK Canada S7N 5A8. Telephone: 306 966-6838; Fax: 306-966-6881;

e-mail: pmh936@mail.usask.ca

AKNOWLEDGMENTS:

This study was supported by Discovery Grant 2383-Huang of the Natural Sciences and Engineering Research Council of Canada, and the Italian Ministry of University and Research (MIUR), PRIN Project.

Impact of Structural Perturbation of Aluminum Hydroxides by Tannate on Arsenate Adsorption

ABSTRACT

The impacts of the biomolecule-induced structural perturbation of Al hydroxides and the resultant alteration of their surface reactivity toward the adsorption of nutrients and contaminants have received, to date, scant attention, in spite of their significance in determining the mineralogy and surface chemistry of these mineral colloids. The present study was aimed to investigate the equilibria and kinetics of arsenate adsorption on a crystalline Al hydroxide, a pure amorphous Al hydroxide and a short-range ordered Al-tannate coprecipitate. Isotherms and kinetics of arsenate adsorption were conducted at pH 6.5; the kinetic experiments (0.083-24 hours) were performed at 288, 298, 308 and 318 K. The adsorption data followed multiple second-order kinetics, with an initial fast reaction step, followed by a slow reaction. While arsenate adsorption on the crystalline Al hydroxide was a rapid process, the poorly ordered minerals required longer contact intervals and greater activation energies. Compared to the pure amorphous Al hydroxide, the incorporation of tannate into the structural network of Al hydroxide decreased the adsorption rate, capacity and the affinity for arsenate. These effects were attributable to the blocking of part of the adsorption sites by tannate, to the electrostatic repulsion induced by the net negative charge caused by the deprotonated organic molecules exposed on the surface of Al-tannate coprecipitate, and to the steric hindrance of tannate, hampering the access of the adsorbate to the micropores. These findings are of fundamental significance in understanding the sorption behavior and mobility of As as influenced by biomolecule-induced structural perturbation of Al hydroxides in the environment.

INTRODUCTION

Arsenic (As) is a toxic metalloid that can cause acute and chronic poisoning involving respiratory, gastro-intestinal, cardio-vascular, nervous and haematopoietic diseases; it may cause skin, renal, liver, bladder and lung cancer (Bissen and Frimmel, 2003). Arsenic can be found in soil and water environments, derived from natural and/or anthropogenic sources. Contaminated ores, sediments, soils and sludges are the main sources of contamination to surface water and groundwater, and possibly to the food chain (Smith et al., 1998; Frankenberger, 2002; Mandal and Suzuki, 2002; Smedley and Kinniburgh, 2002). The "arsenic disaster" in the Bengal basin, resulting from contaminated groundwater, implies a further concern for huge amounts of arsenic that are continuously added to the cultivated soils with the irrigation water (Ali et al., 2003).

Adsorption, precipitation and/or coprecipitation with soil and solution components play important roles in influencing the reactions controlling the equilibria of As between the solid phase and the solution, and hence the mobility of As compounds in soil and water environments. At the concentrations commonly found in soil-water environments, adsorption is a main process controlling the mobility and bioavailability of As in soil-water-plant systems and potentially attenuates As toxic concentration in soil solution, variable charge minerals (Mn, Fe, Al (oxy)hydroxides) being the main adsorbing phases for As in soils (Barrow, 1974; Livesey and Huang, 1981; Oscarson et al., 1981; Nriagu, 1994; Sun and Doner, 1996; Sadiq, 1997; Raven et al., 1998; Goldberg, 2002).

As(III) (arsenite) and As(V) (arsenate) are the forms of As most commonly present in soil. Both As forms are often present in either reduced or oxidized environments because of their relatively slow redox transformation (Sadiq, 1997; Smith et al., 1998). In aerated soils arsenite is oxidized to arsenate that represents the dominating form in aerobic environments,

while under reducing conditions arsenite can be the most representative form (Masschelein et al., 1991).

Several studies have demonstrated that the amount of adsorbed arsenate in soils is correlated with Al and Fe oxides contents (Livesey and Huang, 1981; Goldberg, 1986; Smith et al., 1998; Manning and Goldberg, 1997; Liu et al., 2001, Ladeira and Ciminelli, 2004). The short-range ordered and poorly crystallized oxides, because of their great specific surface and reactivity, can adsorb more As than the crystalline forms, and are reported to be the soil fraction most correlated to arsenic adsorption (Livesey and Huang, 1981; Goldberg, 1986; Goldberg and Johnston, 2001; Violante and Pigna, 2002; De Brouwere et al., 2004). Amorphous Al oxides, in particular, have great adsorption capacity and affinity toward arsenate (Anderson et al., 1976). However, in soil environments, amorphous oxides tend to rapidly evolve to more ordered crystalline forms and the structural perturbation induced by the presences of other soil components, such as biomolecules, have a crucial role in the stabilization of poorly crystalline oxides and in determining the structure and properties of the resulting mineral complexes (Huang and Violante, 1986; Cornell and Shwertmann, 1996; Huang et al., 2002; Violante et al., 2002; Colombo et al., 2004; Yu et al., 2006, 2007). In spite of the wide occurrence in nature of poorly ordered mineral colloids and their great potential for anion retention, very few studies have been devoted to investigate the impact of the biomolecule-induced structural perturbation of oxides on anion adsorption. The presence of organic ligands in metal oxide-organic coprecipitation product can enhance adsorption of heavy metal cations on Al coprecipitates (Yu et al., 2006), and Fe coprecipitates (Liu and Huang, 2003), while the effect on the adsorption of anionic species is poorly understood. The available information are mostly limited to anion adsorption on Fe-organic coprecipitation products (Liu and Huang, 2000; Violante and Pigna, 2002), and very little is known about

anion adsorption on hydrolytic precipitation products of Al formed under the influence of organics (Kwong and Huang, 1978; Huang et al., 2002; Huang, 2008).

Kinetic studies are a useful tool to better understand the rates and processes controlling the adsorption reactions. Arsenic adsorption on Fe and Al oxide is reported as a kinetically fast ligand-exchange reaction (Anderson et al., 1976; Grossl et al., 1997; Raven et al., 1998; Arai and Sparks, 2002) followed by a slower reaction, possibly because of the slow diffusion in micropores (Fuller et al., 1993) or surface reactions, such as surface precipitation (Zhao and Stanforth, 2001) or heterogeneity of the bonding energy of the surface sites (Zhang and Stanforth, 2005). Possible changes in the asorbent-adsorbate affinity because of the coprecipitation of organic ligands with Al in the amorphous structural network would reflect in the rate of adsorption as well as in the adsorption capacity of As, which should have important consequences on the adsorption/desorption equilibria and thus on the environmental mobility of this toxic element. To date, there is no available information on the effect of biomolecule-induced structural perturbation of Al precipitation products on arsenic adsorption. The objective of this work was to investigate the effect of the structural perturbation of Al hydroxides, formed under the influence of tannic acid, on their arsenate adsorption by comparison with pure crystalline and amorphous Al hydroxides.

MATERIALS AND METHODS

Aluminum Precipitation Products

Aluminum precipitation products were prepared as described by Yu et al., (2006). These precipitation products were formed by slowly titrating 7×10^{-3} M $AlCl_3$ solution having initial tannate/Al molar ratios of 0 and 0.1 against 0.1 M NaOH solution up to an OH/Al

molar ratio of 3.0 at a rate of 2.5 mL min^{-1}. Appropriate amount of tannic acid (ACS reagent, $C_{76}H_{52}O_{46}$, FW 1701.20, ignition residue ≤0.5%, Aldrich Chemical Company, Milwaukee, WI) was used to adjust the initial tannate/Al molar ratios in the reaction systems. The suspensions of all the reaction systems were aged for 40 days at 25°C. After aging, the suspensions were filtered by ultrafiltration with a Millipore filter membrane (pore size of 0.1 μm in diameter) and the precipitates were washed with deionized distilled water until the electrical conductivity of the filtrate was less than 5 μS cm^{-1} and free of chloride when tested with 0.1 M $AgNO_3$ solution. The precipitates were finally freeze dried.

A pure amorphous Al hydroxide was synthesized according to Huang et al. (1977). A 0.5 M $AlCl_3$ solution was slowly titrated to pH 7.0 against a 0.5 M NaOH solution. The precipitate was dialyzed against deionized water until it was free of chloride with an electrical conductivity less than 5 μS cm^{-1} and finally freeze dried.

X-ray Diffraction

The Al precipitation products were identified by X-ray diffraction (XRD) with a Rikagu X-ray diffractometer (Model RU 200, Rikagu Co., Tokyo) with Fe-Kα radiation, filtered by a graphite monochromator, at 40kV and 160 mA. The XRD patterns were recorded in the range from 4° to 60° 2θ, with 0.02° 2θ steps at a scanning rate of 10° 2θ per minute.

Surface Properties of the Al-precipitates

The specific surface area of the Al precipitation products was determined by a multiple point Brunauer-Emmett-Teller (BET) N_2 adsorption isotherm (Gregg and Sing, 1982) with an Autosorb 1 (Quantachrome Instruments, Boynton Beach, FL, USA). Prior to N_2 adsorption, 200 mg of the samples were outgassed for 24 h at room temperature and 10 mTorr. During N_2 adsorption, the solid samples were thermostated in liquid N_2 (77-78 K).

The pore specific surface area of the Al precipitation products was determined from the N_2 adsorption isotherm using the t-plot method of de Boer (de Boer et al., 1966; Gregg and Sing, 1982). The specific surface area of the Al precipitation products was also measured by gravimetric methods based on the ethylene glycol monoethyl ether (EGME) (Eltantawy and Arnold, 1973) and water (Quirk, 1955) retention.

The point of zero charge (PZC) of the Al precipitation products and their zeta (ζ) potential and average particle size as a function of the pH were measured on a series of suspensions of 10 samples each with a concentration of 3 g L^{-1} of Al precipitation products prepared in 0.01 M $NaNO_3$ background electrolytic solution and equilibrated for 24 h at 25°C in the pH range from 2 to 12. At the end of the equilibration period, 50 μL of each suspension were transferred to a test tube; the rest of the suspension was centrifuged (2000 × g for 20 min) and 4 mL of each supernatant were used to dilute the respective 50 μL of suspension. The samples were transferred to the test cell and analyzed by Laser Doppler Velocimetry coupled with Photo Correlation Spectroscopy (LDV-PCS) with a photometer DELSA 440, (Beckman Coulter Inc., Fullerton, CA, USA), equipped with a 5 mW He-Ne laser (632.8 nm). The pH was measured potentiometrically at the same time.

All measurements were run in duplicate. The standard deviation of all measurements was determined.

Arsenate Solutions

The arsenate stock solution (13.33 mmol As L^{-1}) was obtained by dissolving bi-sodium arsenate salt ($Na_2HAsO_4 \cdot 7H_2O$; by J.T. Backer Chemicals Co, Phillipsburg, NJ, USA) in 0.01 M $NaNO_3$. Solutions with As concentration in the range between 1.333 and 0.133 mmol L^{-1} were prepared by dilution in 0.01 M $NaNO_3$ before use, and the pH was adjusted at 6.5 with 1 M and/or 0.1 M HCl.

Adsorption Isotherms

The Al-precipitation products were suspended in 0.01 M $NaNO_3$ solution with a suspension density of 1 g L^{-1} and ultrasonified (Sonifier Model 350, Branson, Danbury, CT, USA) at 150 W for 2 min in order to obtain the dispersion of the particles. The pH of the suspensions was adjusted at 6.5 by adding 0.1 M HNO_3 or NaOH and the suspensions were then equilibrated for 24 hours in a Blue M constant temperature shaker bath (Blue M Electronic Co., Blue Island, IL, USA) at 200 rpm and at the temperature of 298 K. The pH of the suspensions was further checked at the end of the preliminary equilibration. Five mL of each suspension were then pipetted into polyethylene test tubes and arsenate solutions at suitable concentrations were added to the respective suspensions to make a final volume of 10 mL. A series of at least six points at increasing As concentrations (from 0 to 0.4 mmol L^{-1}) in 0.01 M $NaNO_3$ was prepared in order to reach the adsorption maximum of each adsorbent, as deduced from preliminary tests. The suspensions were equilibrated for 24 hours at 298 K, and then filtered through Millipore membrane filters (pore size of 0.1 μm). The amount of arsenate in the supernatant was determined colorimetrically according to the method described by Huang and Fujii, (1996). The absorbance of the solution was determined by UV-VIS spectrometer (DU 650, Beckman Coulter Inc., Fullerton, CA, USA) at λ = 840 nm.

The amount of adsorbed As, X_a, in μmol As g^{-1}, was calculated by the following equation:

$$X_a = [(C_0-C_e)\ V]/\ m \qquad (1)$$

where C_0 is the initial As concentration and C_e the residual As concentration (μmol mL^{-1}) at equilibrium; V is the solution volume (mL); and *m* the mass of the adsorbent (g). The experiments were conducted in triplicate.

The experimental error, estimated by Eq. (2) (Thomas et al., 1989), was less than 5%.

$$\Delta X_a/X_a = \Delta C_e/(C_0-C_e) \qquad (2)$$

where ΔX_a is the standard deviation of adsorbed As (X_a) and ΔC_e the standard deviation of the residual As concentration in solution at equilibrium (C_e).

The Langmuir equation (Eq. 3) fitted the adsorption data,

$$X_a = X_{MAX}\, K_L C_e/(1+K_L C_e) \qquad (3)$$

where X_a is the amount of adsorbed As (μmol g^{-1}), C_e is the As concentration at the equilibrium (μmol mL^{-1}), X_{MAX} is the maximum amount of As that may be bound to the adsorbent (adsorption capacity), and K_L is an affinity constant.

Arsenate Adsorption Kinetics

Suspensions of the Al precipitation products with a final density of 0.5 g L^{-1} in 0.01 M $NaNO_3$ at pH 6.5 were prepared as described above and pre-equilibrated for 24 hours at 288, 298, 308 or 318 K. An aliquot of arsenate solution previously equilibrated at pH 6.5 was then added to the suspension to obtain a final As concentration of 0.16 mmol L^{-1} in a final volume of 200 mL, and the reaction vessel was immediately re-transferred to the constant temperature bath shaker. At intervals of 0.083, 0.167, 0.250, 0.333, 0.50, 0.67, 1, 2, 4, 8, 12, and 24 hours, 7 mL were rapidly pipetted from the suspension under vigorous stirring and filtered trough 0.1-μm (pore size) Millipore membrane filters within 15 s. The As concentration in the filtrate was determined colorimetrically according to the method of Huang and Fujii (1996). The amount of adsorbed As was calculated by the difference between the initial As concentration

and the As concentration determined in the solution at each time interval. All the experiments were run in duplicate. The equilibrium pH, the ζ potential and average particle size were measured for each adsorbent-adsorbate system at 298 K after 24 h of interaction.

Kinetic models and statistical analysis of the adsorption data

Different kinetic models (the zero-, first- and second-order, Elovich, parabolic diffusion and power function equations) were applied to the adsorption data and the goodness of the fit was evaluated based on the r^2, the level of significance (p) and the standard error (SE). The statistical analysis of the data was done with the SPSS 12 for Windows (SPSS Inc). Overall, the best fit kinetic model was used to determine the kinetic parameters, including the rate constant calculated from the rate equation, the activation energy and pre-exponential factor calculated from the Arrhenius equation. All the obtained kinetic parameters were compared through Least Significant Differences (LSD) values calculated at 95% and 99% confidence levels.

RESULTS AND DISCUSSION

Characterisation of the Al-precipitation Products

A detailed discussion of the effect of tannate on the structural perturbation of Al precipitates has been reported (Yu et al., 2007). The basic structural and surface properties of the adsorbents pertaining to arsenate adsorption are discussed below. The Al precipitation product formed at a tannate/Al molar ratio of 0 and aged for 40 days was a mixture of crystalline bayerite and gibbsite (Fig. 1a), while the freshly precipitated pure Al hydroxide was initially amorphous to X-ray diffraction (aging time 0 days) (Fig 1b). When tannic acid was added at a tannate/Al molar ratio of 0.1, the precipitation product after 40 days of aging

remained amorphous to X-ray (Fig. 1c). The Al-tannate precipitate had the largest BET specific surface area among the Al precipitation products, and was the only one with detectable microporosity (Table 1), whereas the specific surface area of the amorphous Al hydroxide measured by BET N_2 adsorption was the smallest. The very small BET specific surface area obtained for the pure amorphous Al precipitate was possibly the result of the difficulty in out-gassing to remove the water retained in the small pores, and/or the collapsing of the amorphous structure under vacuum. The tannate molecules in the structure of the Al-tannate precipitation product apparently promoted the formation of a more rigid amorphous network than the pure amorphous Al hydroxide. The collapsing of the structure under vacuum was at least partly prevented; this would allow the penetration of the N_2 molecules inside the pores. Gravimetric methods by EGME and water adsorption were thus also employed to compare the specific surface areas of the three Al-precipitation products. According to the results obtained with EGME adsorption, the specific surface area of the aged Al-tannate precipitation product was still the largest among the three Al precipitation products. In contrast, the specific surface of the pure, amorphous Al hydroxide measured by water adsorption was 12% larger than that of the Al-tannate precipitate. The small water molecule could better penetrate into the small pores. The larger values obtained by water adsorption compared to the other methods could be related to capillary condensation of the water inside the porous structures; this would have allowed the overestimation of the specific surface area by water retention. However, this would provide an indirect, although merely qualitative, evidence of the porous structure of the amorphous Al hydroxide.

The point of zero charge (PZC) values of the crystalline and pure amorphous Al-hydroxides were similar and close to pH 10 (Table 1), which was in agreement with the observations of Goldberg and Johnston (2001). However, in the Al-tannate precipitation product, the PZC decreased to pH 4.9, which was very close to the PZSE measurements

reported by Yu et al. (2006). The great decrease in the PZC was attributed to the complexation of Al by tannate and the development of the excess negative charge in the Al-tannate precipitate (Yu et al., 2007). Therefore, at pH 6.5 the ζ potentials of the surfaces before the interaction with arsenate were positive for both the crystalline and amorphous Al hydroxides, and negative for the Al-tannate precipitation product (Table 1). After 24 h of interaction with 0.16 mmol L^{-1} of arsenate, some increase in the pH was observed for the crystalline and amorphous Al hydroxide systems, while the pH did not change in the case of the Al-tannate precipitate, possibly because of the buffering capacity of the organic component (Table 1). The adsorption of arsenate increased the net negative charge shifting the ζ potential to more negative values in all the reaction systems (Table 1), which was in agreement with previous studies (Goldberg and Johnston, 2001).

Arsenate Adsorption Isotherms

The adsorption of arsenate by the three Al precipitation products at pH 6.5 at the end of a 24-h equilibration period were well described by the Langmuir adsorption model (Table 2), although the fitting for the pure crystalline and amorphous Al hydroxides were somewhat better than that for the Al-tannate precipitate. The Langmuir maximum adsorption (X_{MAX}) per unit weight of the Al precipitates followed the decreasing order: pure amorphous Al precipitate > Al-tannate precipitation product > crystalline Al hydroxide. Based on the arsenate adsorption per unit surface area (EGME specific surface area), however, the X_{MAX} value for the crystalline Al hydroxide was just 5% less than that of the amorphous one; while the X_{MAX} value for the Al-tannate precipitate was nearly one-third of those of the two pure Al hydroxides. The Langmuir affinity constant (K_L) values clearly show the effect of the presence of tannate in the structure of the Al precipitate on decreasing the affinity for arsenate adsorption on the Al hydroxides. The K_L value of the Al-tannate precipitate was nearly one

fourth of the one of the crystalline Al hydroxide, and by three orders of magnitude smaller in comparison to the pure amorphous Al hydroxide.

Arsenate is adsorbed on Al oxides via ligand exchange with the hydroxyl/protonated hydroxyl surface groups of the oxide, and bidentate, binuclear complexes are prevalently formed (Arai et al., 2001; Arai and Sparks, 2002). The interaction of the tannic acid with the aluminum hydroxide during its formation apparently partially blocked the reactive sites of the hydroxide for arsenate adsorption (Table 2), both directly, because of the formation of Al-tannate complexes, and indirectly, because of the steric hindrance of the large tannate molecule bound to the surfaces. Moreover, both the crystalline and pure amorphous Al hydroxides exhibited a net positive surface charge at the experimental pH (Table 1), resulting in their electrostatic attraction of the arsenate anions. In contrast, the net negative charge of the Al-tannate coprecipitation product (Table 1) would impose an electrostatic barrier hampering anion adsorption; this would account for the smaller K_L value obtained for arsenate adsorption on the Al-tannate coprecipitate compared with the other adsorbents (Table 2). The decrease in anion adsorption at increasing pH, in particular above the PZC of the mineral adsorbent, is generally attributed to the diminished electrostatic attraction of the anionic species from the increasingly negative surfaces (Anderson et al., 1976; Parfitt, 1978; Arai and Sparks, 2002). Similarly, the hampering effect of surface coverage by organic molecules toward anion adsorption has been partly explained in terms of the formation of an unfavorable electrostatic field around the surfaces (Xu et al., 1988; Grafe et al., 2001). Moreover, the Al-tannate precipitate was microporous (Table 1). The steric hindrance, coupled with the electrostatic repulsion induced by tannate molecules, apparently hampered the access of arsenate especially to the micropores, further reducing the available sorption sites (Table 2). Liu and Huang (2000) found a decrease in phosphate adsorption per unit surface area on Fe hydroxides formed in the presence of different citrate concentrations, and

this effect was attributed to the blocking effect of the organic molecules. Like in the present study, the effect of the organic molecules in increasing the specific surface area induced an increase of the adsorbed anions per unit weight of the adsorbent, compared with the crystalline Fe hydroxide formed in the absence of organic acid. The former, however, adsorbed less anions per unit surface area compared with the latter. The comparison of the X_{MAX} and K_L values of As adsorption by the pure, amorphous Al hydroxide and Al-tannate precipitation product further indicated the inhibiting effect of the coprecipitated tannate on As adsorption on Al precipitates (Table 2). This effect may depend on the nature of the organic ligand, as suggested by the results obtained by Kwong and Huang (1981) and De Cristofaro et al., (2000) on phosphate adsorption on organic-perturbed Al precipitates.

Kinetics of Arsenate Adsorption

The adsorption of arsenate on both the crystalline and pure amorphous Al hydroxides was a fast reaction; the amount of arsenate adsorbed during the first 5 min accounted for 69 ± 0.2% and 57 ± 0.1% of the arsenate adsorbed by the former and latter, respectively, at the end of a 24-h equilibration period (Table 3). The arsenate adsorption on the Al-tannate precipitate was much slower; only 14 ± 0.9% of the arsenate adsorbed at the end of 24 h was adsorbed within the first 5 min. After 30 min, 79 ± 0.7%, 73 ± 0.1% and 30 ± 0.8% of the As adsorbed at the end of 24 h were adsorbed by the crystalline Al hydroxide, pure amorphous Al hydroxide and Al-tannate precipitate, respectively. The total amount of arsenate adsorbed by the Al-tannate precipitate at the end of the 24-h reaction period at 298 K was smaller than the amount adsorbed by the crystalline Al hydroxide (Table 3), although the X_{MAX} (mmol kg^{-1}) calculated from the Langmuir equation was larger for the former than the latter (Table 2). This was attributed to the greater affinity of the crystalline Al hydroxide for arsenate adsorption, compared with the Al-tannate precipitate, resulting in larger arsenate adsorption

on the crystalline Al hydroxide at the more dilute As concentrations such as the one used in the kinetic experiment. The Al-tannate precipitate adsorbed larger amounts of arsenate than the crystalline Al hydroxide only when As was added at concentrations above 0.2 mM, as observed in the adsorption isotherms (data not shown). At the As concentration used in the kinetic study, it appeared that, besides the initial As activity, the microporosity and the net negative surface charge of the Al-tannate precipitate (Table 1) retarded the kinetics of arsenate adsorption.

In agreement with the present results, in a study conducted by Anderson et al., (1976), 90% of the As adsorbed at equilibrium by an amorphous Al hydroxide was subtracted from the solution during the first 5 min. The chemical reactions of surface adsorption are fast reactions, occurring within milliseconds, (as shown by Grossl et al., 1997, for the formation of the arsenate-goethite inner sphere complex), whereas the diffusion-controlled processes are much slower and can be measured with batch experiments (Sparks, 1989). The even more rapid approaching of the equilibrium with most of the As adsorbed by the crystalline Al hydroxide within the first 5 min indicated that the adsorption of arsenate on the crystalline Al hydroxide was less limited by intraparticle diffusion processes than that on the amorphous Al hydroxide and especially that on the Al-tannate precipitate (Table 3).

The complete reaction period (between 0.083 and 24 hours) could be described by Elovich equation for all the three systems ($r^2 \geq 0.995$; $SE \leq 4.0 \times 10^{-1}$; $p \leq 4.6 \times 10^{-8}$). Although Elovichian kinetics could account for diffusion-controlled processes, there is no direct relationship between the adsorption mechanisms and the model giving the best fitting (Sparks, 1989; Aharoni et al., 1991), and Elovich equation can describe a number of different processes (Zhang and Stanforth, 2005). Moreover, when heterogeneous surfaces are involved, several mechanisms can contribute to the overall process and it is possible that different mechanisms can dominate the adsorption reaction at different times, and then the adsorption

rate as well as the rate-limiting process can vary during the time (Strawn and Sparks, 1999). In the present study, after the fast step (0 to 0.5 hours), the reaction became slower, and a quasi equilibrium was reached within 24 hours (Fig. 2), in accord with the observations of Anderson et al. (1976).

This biphasic behavior of arsenate adsorption has been observed in several studies on pure Al and Fe oxides (Fuller et al., 1993; Raven et al., 1998; O'Reilly et al., 2001; Arai and Sparks 2002) and soils (Livesey and Huang, 1981; Smith et al., 1999; Zhang and Selim, 2005). The biphasic rate processes have also been reported for the adsorption kinetics of different anions such as phosphate and selenite (Liu and Huang, 2000; Saha et al., 2004) and cations, such as Pb and Cd (Liu and Huang, 2003; Yu et al., 2006) and are generally attributed to the heterogeneity in the adsorption sites with different binding strength and different accessibility inside the pores. In the present case, besides the increasing of the negative charge of the surface as the adsorption proceeded, the heterogeneity could have been the result of the different reactivities at the adsorption sites, and of the different accessibility to pores of different sizes in the noncrystalline samples when compared with the crystalline one.

On the basis of the steepness of the adsorption curves, the adsorption kinetics of arsenate on the three Al precipitates could thus be divided into a fast-reaction step (0.083-0.5 hours) followed by a slower reaction (0.5 to 12 hours). The kinetic and empirical equations, including the zero-, first- and second-order rate equations, the Elovich equation, parabolic diffusion and power function equations were applied to the fast and slow steps of the adsorption reaction. The statistical results from the regressions, including the determination coefficient (r^2), significance (p) of the regression analysis and standard error (SE) for the fast and slow adsorption reactions of arsenate on the three Al precipitates at 298 K are shown as an example in Table 4. The empirical equations (the Elovich, parabolic diffusion and power function) gave good fittings ($r^2 > 0.96$). Although the Elovich equation was found to

adequately describe anion adsorption on soils and soil minerals (Chien and Clayton, 1980; Elkhatib et al., 1984; Torrent, 1987; Zhao and Stanforth, 2001; Zhang and Stanforth, 2005), it does not provide well defined physicochemical parameters, which is also true for the power-function equation (Aharoni et al., 1991; Sparks, 2003). The parabolic diffusion equation was found to properly describe arsenic adsorption on ferrihydrite (Raven et al., 1998), and it is often used to determine whether a process is diffusion controlled; however, it only provides an "apparent" diffusion rate (Sparks, 1989; Ho et al., 2000). Complex multi-controlled mechanisms could give similar results when fitted by different models and the good statistical fit could not discriminate between the kinetics and the mechanism involved (Galwey, 2003). There is no consistent relationship between the equation giving the best fit, and the nature of the adsorption process actually involved. Dissimilar processes can conform to the same equation or, vice versa, similar processes can be fitted by different equation (Aharoni et al., 1991; Galwey, 2003). Nevertheless, the parameters of the chosen model can provide some meaningful tools to compare the rates of the adsorption processes on different adsorbents (Liu and Huang, 2000; Saha et al., 2004) at least under the same experimental conditions. Comparing the fit to the zero-, first- and second-order rate equations to the kinetic data, the second-order rate equation was found to better describe the adsorption data, according to all the tested statistical parameters, for both the fast and slow steps of the adsorption kinetics at 298 K (Table 4), as well as at other three temperatures studied (data not shown). Similarly, phosphate adsorption on Fe oxides and selenite adsorption on hydroxy-Al-montmorillonite complexes were found to be properly described by a second order rate equation (Liu and Huang, 2000; Saha et al., 2004). Thus, a multiple second-order rate equation was chosen to determine the rate constants and the temperature dependence of arsenate adsorption. Linear plots obtained for the 298 K data set are shown in Fig. 3 as an example.

In the temperature range studied, the rate constants for arsenate adsorption on the three adsorbents, both in the fast and the slow reaction, generally varied in the order of amorphous Al hydroxide >> Al-tannate precipitate ≥ crystalline Al hydroxide (Table 5). There was no significant difference in the rate constants for the fast reaction for arsenate adsorption between the crystalline Al hydroxide and the Al-tannate precipitate in the temperature range studied. The rate constants for the slow reaction for arsenate adsorption by the crystalline Al hydroxide and those for the slow reaction of arsenate adsorption by the Al-tannate precipitate at 288 and 298 K also did not significantly differ. However, the rate constants showed that the reaction rates of the slow reaction of arsenate adsorption by the Al-tannate precipitate were 40% and 52% faster than those of the slow reaction of arsenate adsorption by the crystalline Al hydroxide at 303 and 318 K, respectively. This indicated that a high temperature was needed to overcome the energy barriers for the former than the latter. The increase in the temperature generally resulted in an increase of the adsorption rates, because of the increased energy available to enhance the diffusion of the adsorbate, and to allow the breaking and formation of bonding at the surface of the Al hydroxides (Sparks, 1989; Liu and Huang, 2000; Saha et al., 2004; Yu et al., 2006). However, the temperature dependence of the adsorption rate constants within the fast (or slow) reaction varied with the different Al precipitates (Fig. 2 and Table 5). The rate constants of arsenate adsorption on the crystalline Al hydroxide in the fast reaction only showed an increasing trend with the increasing of the temperature. By contrast, the rate constants of the fast reaction for the pure amorphous Al precipitate at 318 K was increased by a factor of 2.7 compared with the value found at 288 K and for the Al-tannate precipitate the increase was by a factor of 3.9. During the slow reaction, the rate constants for the amorphous Al hydroxide showed the highest temperature dependence, increasing by a factor of 10.7 from 288 K to 318 K, whereas the rate constant for the Al-

tannate precipitate was increased by a factor of 3.4 and the crystalline Al hydroxide did not show temperature dependence in this last phase of the adsorption reaction.

The little temperature dependence of arsenate adsorption on the crystalline Al hydroxide observed in the studied time interval (Table 5) was attributed to the absence of micropores (Table 1), the smooth surfaces with few structural defects of the crystalline structure, and the exposed net positive charge of the reactive sites on the surface (Table 1). Therefore, the crystalline Al hydroxide would readily interact with arsenate anions in solution. Most of the adsorption process in the crystalline Al hydroxide system actually occurred within the first 5 min (Table 3). Compared with the amorphous material, arsenate adsorption was more rapid in the crystalline Al hydroxide system (Table 3). For the amorphous adsorbents, the reactive sites were apparently less directly exposed to the adsorbate, especially for the microporous Al-tannate precipitate (Table 1), where the amount of As adsorbed at 5 min only accounted for 14 ± 0.9% As adsorbed after 24 h (Table 3). In this case the increased energy availability at increased temperature was more effective in promoting the adsorption rate (Table 5) by enhancing intraparticle diffusion in the micropores and overcoming the electrostatic repulsion between arsenate and the negatively charged surfaces of the Al-tannate precipitate (Table 1).

Comparing the rate constants for the fast and slow steps of arsenate adsorption on the three adsorbents, the differences between the rate constants of the fast and slow steps decreased in the order: crystalline Al hydroxide > Al-tannate precipitate > amorphous Al hydroxide (Table 5). The fast reaction was faster than the slow reaction by one order of magnitude for the crystalline Al precipitation product, and by a factor of 5 for the Al-tannate precipitate at the four temperatures. For the amorphous Al hydroxide, the differences between the fast and slow steps tended to disappear at increasing temperatures (the ratio between rate constants of the fast and slow reactions varied from 4.5 at 288 K to 1.1 at 318 K), indicating a

greater temperature dependence of the slow reaction compared with the fast one for this adsorbent. Although there was no measurable BET micropore surface area by N_2 adsorption for the amorphous Al hydroxide, its larger specific surface area obtained with water adsorption (Table 1) compared with the other methods indicated that this material could have a microporous structure, which may be unstable under a high-vacuum condition. The access of the adsorbate to the small pores would require a higher energy and a longer induction period; also the increased temperature would enhance the mobility of the adsorbate inside the micropores (Liu and Huang, 2000). After arsenate could access to the micropores, the strong affinity of arsenate to the adsorbent would account for the rapid surface interaction between the Al hydroxide and the arsenate anions. The fact that the differences between the fast and slow reactions in the case of the Al-tannate precipitate remained almost constant for all the four experimental temperatures (Table 5) could be attributed to a more constant energy requirement for arsenate adsorption on this substrate; this may be linked to an electrostatic barrier caused by the negative charge induced by the coprecipitated organic molecules besides the slow diffusion inside the micropores because of steric factors.

Activation Energy and Pre-exponential Factor

The effect of the temperature on the adsorption of arsenate on the three Al precipitates was further investigated by the use of the Arrhenius equation (Eq. 4) (Moore and Pearson, 1981) for the determination of the energy of activation and the pre-exponential factor:

$$k = A\, e^{-Ea/RT} \qquad (4)$$

where k is the rate constant, A is the pre-exponential factor (frequency factor), E_a is the Arrhenius energy of activation, R is the universal gas molal constant (8.314 J K^{-1} mol^{-1}), and T is the absolute temperature (K). The Arrhenius energy of activation and the pre-exponential factor can be calculated from the slope and intercept, respectively, of plots of ln k versus 1/T.

The linear plots of the data to Arrhenius equation are illustrated in Fig. 4. The temperature dependence of arsenate adsorption by the crystalline Al hydroxide was apparent only in the fast reaction. Both the fast and slow reactions of the adsorption process on the pure amorphous Al hydroxide and on the Al-tannate precipitate were well described by Arrhenius equation, with r^2 values ranging between 0.962 and 0.999 ($p < 0.05$). The E_a value (Table 6) calculated for arsenate adsorption on the crystalline hydroxide in the fast adsorption process was only 8 kJ mol^{-1} arsenate adsorbed. The E_a values for the fast reaction of arsenate adsorption on the amorphous Al hydroxide and on the Al-tannate precipitate were 26 and 34 kJ mol^{-1} arsenate adsorbed, respectively. Reported E_a values for film diffusion are typically less than 25 kJ mol^{-1} and reported values for intraparticle diffusion processes are in the range 21 to 42 kJ mol^{-1} (Sparks, 1999). Thus, the E_a values less than 42 kJ mol^{-1} indicate that diffusion-controlled processes are the rate-limiting step in the reaction, whereas greater E_a values can account for chemically controlled processes as the rate-limiting step (Sparks, 1999). The obtained data (Table 6), thus, indicated that diffusion processes were the rate-limiting step in the arsenate adsorption by the three adsorbents with the exception that the chemically controlled process, which involved bond breaking and formation, was the rate-limiting step in the slow reaction of arsenate adsorption by the amorphous Al hydroxide (48 kJ mol^{-1}). This could be attributed to greater energy required for arsenate to react with adsorption sites (Table 6) with a greater degree of structural defects on the more extensively damaged surfaces characterizing the amorphous and poorly ordered Al precipitates compared with the crystalline Al hydroxides (Kwong and Huang, 1979).

Liu and Huang (2000) found a heat of activation of 97 kJ mol $^{-1}$ of phosphate adsorbed on iron hydroxides formed at a Fe/citrate molar ratio 0.1, indicating a chemical rate-limiting step, which was attributed to the ligand exchange of citrate by phosphate. In the Al-tannate precipitates the organic molecules were incorporated in the structure of the poorly ordered precipitation product (Colombo et al., 2004; Yu et al., 2006), with a fibrous morphology (Colombo et al., 2004). Thus, the exchange of the larger tannate molecules with arsenate was apparently more difficult. The energy of activation for the slow reaction of cadmium adsorption on the same Al-tannate precipitation product was also in the range of chemically controlled processes (Yu et al., 2006); however the presence of the organic molecules and the resultant microporosity and net negative charge of the Al-tannate precipitate (Table 1) at the experimental pH had different effects on the adsorption of cationic (Yu et al., 2006) and anionic (Table 6) species. The similar E_a values of the fast and slow reactions of arsenate adsorption by this adsorbent indicated that a similar, diffusion-controlled process limited both reaction steps in the Al-tannate precipitate system.

The pre-exponential factor gives an indication of the accessibility of the adsorbate ions to the surfaces (Liu and Huang, 2000) and the collision frequency of the adsorbate with the reactive sites of the adsorbent (Saha et al., 2004). The pre-exponential factor values (Table 6) obtained for the fast reaction of arsenate adsorption on the three Al precipitates were in the order: Al-tannate precipitate ≈ amorphous Al hydroxide > crystalline Al hydroxide. This could be explained by a larger number of reactive and accessible sites on the Al-tannate precipitate and pure amorphous Al hydroxide compared with the crystalline one. In the amorphous Al precipitation product, a larger amount of exposed Al-OH and Al-OH_2 groups on the edges and corners of the disordered structure were likely available for specific adsorption (Kwong and Huang, 1978 and 1981; Huang and Violante, 1986; De Cristofaro et al., 2000; Saha et al., 2004; Yu et al., 2006). Although the poorly ordered structure of the Al-

tannate precipitate had been stabilized during the aging period (Fig. 1), compared with the pure amorphous Al hydroxide, some of the exposed Al-OH_2 and –OH groups might be blocked by the tannate molecules by ligand exchange reactions and part of the reactive sites situated inside the micropores (Table 1) might not be accessible to the arsenate ions because of steric hindrance. Furthermore, the unfavorable electrostatic charge (Table 1) resulting from the incorporation of tannate ligands into the amorphous structural network might also hinder the contact between the binding sites on the Al hydroxides surface and the anionic adsorbate. While exposed carboxyl and phenolic hydroxyl functional groups can act as potential adsorption sites for cations, such as calcium (Kwong and Huang, 1981) and cadmium (Yu et al., 2006), the presence of dissociated carboxyl and phenolic hydroxyl groups would increase the negative charge and thus hamper anion adsorption. During the fast reaction, both a lesser energy of activation required and a similar frequency factor (Table 6) can account for the greater rate constant (Table 5) for arsenate adsorption on the pure amorphous Al hydroxide when compared with the Al-tannate precipitation product. In the slow reaction, however, the activation energy was greater for the pure amorphous Al hydroxide when compared with the Al-tannate precipitate, and the greater rate constant of the former than the latter can be explained only by the increased frequency factor. The smaller frequency factor for the slow reaction of arsenate adsorption by the Al-tannate precipitate was attributed to the decrease of accessible reaction sites.

CONCLUSIONS

The stabilization of the poorly ordered structure of Al hydroxides by coprecipitated organic molecules, such as tannic acid, substantially affects the surface properties of the Al precipitation product. Besides the long-term preservation of a large specific surface area and

porosity, the organic component substantially shifts the PZC toward more negative values. While pure amorphous Al hydroxides would rapidly evolve toward more crystalline forms, the organically stabilized amorphous Al hydroxides would persist in soil and related environments (Huang et al., 2002). However, although the organic stabilization of the short-range ordered structure of Fe and Al oxides substantially enhances cation adsorption (Kwong and Huang, 1981; Liu and Huang, 2001 and 2003; Yu et al., 2006), the implications on anion adsorption depend on the organic C content and the nature of the organics incorporated in the precipitates (Kwong and Huang, 1978 and 1981; Liu and Huang, 2000). The present work showed that the structural perturbation of Al hydroxides by tannate and the resulted alteration of the surface characteristics of these hydroxides caused a substantial modification of their kinetics and equilibria of arsenate adsorption.

Among the three Al precipitation products, the amorphous Al hydroxide formed in the absence of tannate had the greatest Langmuir adsorption maximum on a weight basis and chemical affinity for arsenate. Although the Langmuir adsorption maximum on a weight basis of the Al precipitate formed at a tannate/Al molar ratio of 0.1 was greater than that of the crystalline Al hydroxide formed in the absence of tannate, the chemical affinity of the former for arsenate was smaller than that of the latter. The rate constants of the arsenate adsorption were generally in the order: amorphous Al hydroxide >> Al-tannate precipitate ≥ crystalline Al hydroxide, which was governed by the activation energy and frequency factor of the reaction. In the slow reaction, the rate constants of the arsenate adsorption on the Al-tannate precipitate at higher temperatures were significantly greater than those of the crystalline Al hydroxide, indicating that more energy was needed to overcome the energy barrier for arsenate anions to approach the negatively charged surfaces and the reactive sites in the micropores of the Al-tannate precipitate. The blocking of part of the active Al-HO and $-H_2O$ sites by the tannate by ligand exchange reactions and the steric hindrance of the large organic

molecules would hamper the access of the adsorbate into the small pores. These processes were also considered important in contributing to slow the intraparticle diffusion of arsenate to the active sites at the internal surface of the porous structure. Therefore, a longer reaction period was required to attain arsenate adsorption equilibrium in the Al-tannate precipitate reaction system. Based on the characteristics of structural and surface properties of Al precipitates and the Langmuir parameters and kinetic data of arsenate adsorption by these precipitates, the impacts of the structural perturbation of an oxide by biomolecules and the resultant alteration of their surface reactivity toward anions would depend on the balance of counteracting effects: (1) a large specific surface area developed as a result of the structural perturbation and a large density of structural defects with a high-energy surface that could, thus, act as active sites for the adsorption on one hand, and (2) the degree of incorporation of the biomolecules into the oxide structural network and the resultant modification of reactive sites, surface charge, and steric factor on the other hand. The results should also vary with the nature of the oxides/hydroxides, biomolecules and adsorbates involved.

The present findings are of fundamental significance in understanding the dynamics and fate of arsenic as influenced by short-range ordered Al hydroxides formed under the influence of biomolecules in the environment.

REFERENCES

Ali, M.A., A.B.M. Badruzzaman, M.A. Jalil, M.D. Hossain, M.F., Ahmed, A. Al Masud, Md. Kamruzzaman, and M.A. Rahman. 2003. Fate of arsenic extracted with groundwater. *In* Fate of arsenic in the environment, BUET-UNU International Symposium Proceedings, M.F Ahmed, M. Ashraf Ali and Z. Adeel (eds.), 5-6 February 2003, Dhaka, Bangladesh. ITN Centre, BUET (Dhaka), and The United Nations University (Tokyo), pp 7-20.

Aharoni, C., D.L. Sparks, S. Levinson, and I. Ravina. 1991. Kinetics of soil chemical reactions: relationship between empirical equations and diffusion models. Soil Sci. Soc. Am. J. 55: 1307-1312.

Anderson, M.A., J.P. Ferguson, and J. Gavis. 1976. Arsenate adsorption on amorphous aluminum hydroxide. J. Colloid Interface Sci. 54: 391-399.

Arai Y., E.J. Elzinga and D.L. Sparks. 2001. X-ray adsorption spectroscopic investigation of arsenite and arsenate adsorption at the aluminum oxide-water interface. J. Colloid Interface Sci. 235: 80-88.

Arai, Y., and D.L. Sparks. 2002. Residence time effect on arsenate surface speciation at the aluminum oxide-water interface. Soil Sci. 167: 303-314.

Barrow, N.J. 1974. On the displacement of adsorbed anions from soil: 2. Displacement of phosphate by arsenate. Soil Sci. 117: 28-33.

Bissen, M. and Frimmel, F.H. 2003. Arsenic, a review. Part I: occurrence, toxicity, speciation, mobility. Acta Hydrochim. Hydrobiol. 31: 9–18.

Chien, S.H. and W.R. Clayton. 1980. Application of Elovich equation to the kinetics of phosphate release and sorption in soils. Soil Sci. Soc. Am. J. 61: 772-783.

Colombo, C., M. Ricciardella, A. Di Cerce, L. Maturo, and A. Violante, 2004. Effects of tannate, pH, sample preparation, ageing and temperature on the formation of and nature of Al oxyhydroxides. Clays Clay Miner. 52: 721-733.

Cornell, R.M. and U. Schwertmann, 1996. The iron oxides. VCH - Verlagsgesellschaft, Weinheim, New York

de Boer, J.H., B.C. Lippens, B.G. Linsesn, J.P. Broeckhoff, A. Heuval, and T.J. Osinga. 1966. The *t*-curve of multilayer N_2-adsorption. J. Colloid Interface Sci. 21: 405-414.

De Brouwere, K., E. Smolders and R. Merckx. 2004. Soil properties affecting solid-liquid distribution of As(V) in soils. Eur. J. Soil Sci. 55: 165–173.

De Cristofaro, A., J.Z. He, D.H. Zhou and A. Violante. 2000. Adsorption of phosphate and tartrate on hydroxy-aluminum-oxalate precipitates. Soil Sci. Soc. Am. J. 64: 1347-1355.

Elkhatib, E.A., O.L. Bennett, and R.J. Wright. 1984. Kinetics of arsenite adsorption in soils. Soil Sci. Soc. Am. J. 48: 758-762.

Eltantawy, I.M. and P.W. Arnold, 1973. Reappraisal of ethylene glycol monoethyl ether (EGME) method for surface area estimation of clays. J. Soil Sci. 24: 232-238.

Frankenberger, W. T., Jr. (ed.). 2002. Environmental chemistry of arsenic. Marcel Dekker, New York.

Fuller, C.C., J.A., Davis and G.A. Waychunas 1993. Surface chemistry of ferrihydrite: Part 2. Kinetics of arsenate adsorption and copricipitation. Geochim. Cosmochim. Acta. 57: 2271-2282.

Galwey, A.K. 2003. Eradicating erroneous Arrhenius arithmetic. Thermochim. Acta, 399: 1-29.

Goldberg, S. 1986. Chemical modeling of arsenate adsorption on aluminium and iron oxide minerals. Soil Sci. Soc. Am. J. 50: 1154-1157.

Goldberg S., and C.T. Johnston. 2001. Mechanisms of arsenic adsorption on amorphous oxides evaluated using macroscopic measurements, vibrational spectroscopy and surface complexation modeling. J. Colloid Interface Sci. 234: 204-216.

Goldberg S. 2002. Competitive adsorption of arsenate and arsenite on oxides and clay minerals. Soil Sci. Soc. Am. J. 66: 413-421.

Grafe, M., M.J. Eick, and P.R. Grossl. 2001. Adsorption of arsenate (V) and arsenite (III) on goethite in the presence and absence of dissolved organic carbon. Soil Sci. Soc. Am. J. 65: 1680-1687.

Gregg, S.J. and K.S.W. Sing. 1982. Adsorption, surface area and porosity. 2nd edition. Academic Press Inc, London.

Grossl, P.R., M., Eick, D.L. Sparks, S. Goldberg and C.C. Ainsworth. 1997. Arsenate and chromate retention mechanisms on goethite. 2. Kinetic evaluation using a pressure-jump relaxation technique. Environ. Sci. Technol. 31: 321-326.

Ho, Y.S., J.C.Y. Ng, and G. McKay. 2000. Kinetics of pollutants sorption by biosorbents: review. Separation Purif. Methods 29: 189-232.

Huang, P.M. 2008. Impacts of physicochemical and biological interactions on metal and metalloid transformations in soils: an overview. *In* A. Violante, P.M. Huang and G.M. Godd (eds) Biophysico-chemical processes of heavy metals and metalloids in soil environments. Vol. I, Wiley-IUPAC Series in Biophysico-Chemical Processes in Environmental Systems. John Wiley and Sons, Hoboken, N.J., pp 3-52.

Huang, P.M., T.S.C. Wang, M.K. Wang, M.H. Wu, and W. Hsu. 1977. Retention of phenolic acids by noncrystalline hydroxy–aluminum and –iron compounds and clay minerals of soils. Soil Sci. 123: 213-219.

Huang, P.M. and A. Violante. 1986. Influence of organic acids on crystallization and surface properties of precipitation products of aluminum. *In* P.M. Huang and M. Schnitzer (eds) Interactions of soil minerals with natural organics and microbes. SSSA Spec. Pub. 17, SSSA, Madison, WI. pp 159-221.

Huang, P.M. and R. Fujii. 1996. Selenium and arsenic. *In* D.L. Sparks (ed.) Methods of soil analysis. Part 3. Chemical methods. SSSA Book series no 5. SSSA, Madison, WI. pp 793-831.

Huang P.M., M.K. Wang, N. Kampe, and D.G. Schulze. 2002. Aluminum hydroxides. *In* J.B. Dixon and D.G. Schulze (eds) Soil Mineralogy with environmental applications. SSSA Book Series, no.7. SSSA, Madison, WI. pp. 261-289.

Kwong, K.F.N.K and P.M. Huang. 1978. Sorption of phosphate by hydrolytic reaction products of aluminum. Nature 5643: 336-338.

Kwong, K.F.N.K and P.M. Huang. 1979. Nature of hydrolytic precipitation products of aluminum as induced by low-molecular-weight complexing organic acids. *In* M.M. Mortland and V.C. Farmer (Eds.), Proceedings of the VI International Clay Conference 1978. Elsevier Scientific Publishing Company, Amsterdam, the Netherlands. pp. 527–536.

Kwong, K.F.N.K. and Huang, P.M. 1981. Comparison of the influence of tannic acid and selected low molecular weight organic acids on precipitation products of aluminium. Geoderma 26: 179-193.

Ladeira, A.C.Q. and V.S.T. Ciminelli. 2004. Adsorption and desorption of arsenic on an oxisol and its constituents. Water Research. 38: 2087-2094.

Liu C. and P.M. Huang. 2000. Kinetics of phosphate adsorption on iron oxides formed under the influence of citrate. Can J. Soil Sci. 80:445-454.

Liu, F., A. De Cristofaro, and A.Violante. 2001. Effect of pH, phosphate and oxalate on the adsorption/desorption of arsenate on/from goethite. Soil Sci. 166: 197-208.

Liu, C. and P.M. Huang. 2001. Pressure-jump relaxation studies on kinetics of lead sorption by iron oxides formed under the influence of citric acid. Geoderma 102: 1-27.

Liu C. and P. M. Huang. 2003. Kinetics of lead adsorption by iron oxides formed under the influence of citrate. Geochim. Cosmochim. Acta 67: 1045-1054.

Livesey, N.T., and P.M. Huang. 1981. Adsorption of arsenate by soils and its relation to selected chemical properties and anions. Soil Sci. 131: 88-94.

Mandal, B.K. and Suzuki, K.T. 2002. Arsenic round the world: a review. Talanta 58: 201-235.

Manning, B.A. and S. Goldberg. 1997. Adsorption and stability of arsenic (III) at the clay mineral-water interface. Environ. Sci. Technol. 31: 2005-2011.

Masschelein, P.H., R.D. Delaune and W.H. Patrick, Jr. 1991. Effect of redox potential and pH on arsenic speciation and solubility in a contaminated soil. J. Environ. Qual. 25: 1414-1419.

Moore, J.W. and R.G. Pearson. 1981. Kinetics and mechanisms. 3rd ed. John Wiley and Sons, New York, NY, USA.

Nriagu, J.O. 1994. Arsenic in the environment. Part I. Adv. Environ. Sci. Technol. 26. John Wiley & Sons, New York, USA.

O'Reilly, S.E., D.G. Strawn and D.L. Sparks. 2001. Residence time effect on arsenate adsorption/desorption mechanisms on goethite. Soil Sci. Soc. Am. J. 65: 67-77.

Oscarson, D.W., P.M. Huang, and W.K. Liaw. 1981. Role of manganese in the oxidation of arsenite by freshwater lake sediments. Clays Clay Miner. 29:219-225.

Parfitt, L.R. 1978. Anion adsorption by soils and soil minerals. Adv. Agron. 30:1-50.

Quirk, J.P. 1955. Significance of surface areas calculated from water vapour sorption isotherms by use of the B.E.T. equation. Soil Sci. 80: 423-430.

Raven, K., A. Jain, and R. H. Loeppert. 1998. Arsenite and arsenate adsorption on ferrihydrite: kinetics, equilibrium, and adsorption envelopes. Environ. Sci. Technol. 32: 344-349.

Sadiq, M. 1997. Arsenic chemistry in soils: an overview of thermodynamic predictions and field observations. Water Air Soil Pollut. 93: 117-136.

Saha, U.K., C. Liu, L.M. Kozak, and P.M. Huang. 2004. Kinetics of selenite adsorption on hydroxyaluminum- and hydroxyaluminumsilicate-montmorillonite complexes. Soil Sci. Soc. Am. J. 68: 1197-1209.

Smedley, P.L., and D.G. Kinniburgh. 2002. A review of the source, behaviour and distribution of arsenic in natural waters. Appl. Geochem. 17: 517-568.

Smith, E., R. Naidu, and A.M. Alston. 1998. Arsenic in the soil environment: a review. Adv. Agron. 64: 149-195.

Smith, E., R. Naidu, A. M. Alston. 1999. Chemistry of arsenic in soils: I. Adsorption of arsenate and arsenite by selected soils. J. Environ. Qual. 28: 1719-1726.

Sparks, D.L. 1989. Kinetics of soil chemical processes. Academic Press, New York, NY, USA.

Sparks, D.L. 1999. Kinetics of sorption/release reactions at the soil mineral/water interface. *In* Sparks, D.L. (Ed). Soil Physical Chemistry, 2nd ed. CRC Press, Boca Raton, FL, USA, pp 135-191.

Sparks, D.L. 2003. Environmental soil chemistry, 2nd ed. Academic Press, New York, NY, USA.

Strawn, D.G. and D.L. Sparks. 1999. Sorption kinetics of trace elements in soils and soil minerals. *In* Selim, H.M. and Iskandar I.K. (eds.) Fate and transport of heavy metals in the vadose zone. Lewis Publisher, Boca Raton, FL, USA. pp. 1-15.

Sun, X., and H.E. Doner. 1996. An investigation of arsenate and arsenite bonding structures on goethite by FTIR. Soil Sci. 161: 865-872.

Thomas, F., J.Y. Bottero and J.M. Cases. 1989. An experimental study of the adsorption mechanisms of aqueous organic acids on porous aluminas. 1. The porosity of the

adsorbent: A determining factor for the adsorption mechanisms. Colloid Surf. 37: 269-280.

Torrent, J. 1987. Rapid and slow phosphate sorption by Mediterranean soils. Effect of iron oxides. Soil Sci. Soc. Am. J. 51: 78-82.

Violante A. and M. Pigna. 2002. Competitive sorption of arsenate and phosphate on different clay minerals and soils. Soil Sci. Soc.Am. J. 66: 1788-1796.

Violante, A., G.S.R. Krishnamurti, and P.M. Huang, 2002. Impact of organic substances on the formation and transformation of metal oxides in soil environments. *In* P. M. Huang, J.-M. Bollag and N. Senesi (eds.) Interactions between soil particles and microorganisms. John Wiley & Sons, Chichester, UK pp 133-171.

Xu, H., B. Allard and A. Grimvall. 1988. Influence of pH and organic substances on the adsorption of As(V) on geological materials. Water Air Soil Pollut. 40: 293-305.

Yu, G., U.K. Saha, L.M. Kozak and P.M. Huang. 2006. Kinetics of Cd adsorption on aluminum precipitation products formed under the Influence of tannate. Geochim. Cosmochim. Acta 70: 5134-5145.

Yu, G., U.K. Saha, L.M. Kozak and P.M. Huang. 2007. Combined effects of tannate and ageing on structural and surface properties of aluminum precipitates. Clays Clay Miner. 55: 369-379.

Zhang, H. and H.M. Selim. 2005. Kinetics of arsenate adsorption-desorption in soils. Environ. Sci. Techol. 39: 6101-6108.

Zhang, J. and R. Stanforth. 2005. Slow adsorption reaction between arsenic species and goethite (α-FeOOH): diffusion or heterogeneous surface reaction control. Langmuir, 21: 2895-2901.

Zhao, H., and R. Stanforth. 2001. Competitive adsorption of phosphate and arsenate on goethite. Environ. Sci. Technol. 35: 4753-4757.

List of Figures

Table1. Selected surface characteristics of the Al precipitation products before and after arsenate adsorption (24 h of interaction at 25°C).

		[†]Crystalline Al hydroxide	[‡]Amorphous Al hydroxide	[†]Al-tannate precipitate
		Before arsenate adsorption		
BET Specific surface area	*(m^2 g^{-1})*	49 ± 8[§]	20 ± 4	169 ± 2
Micropore area	*(m^2 g^{-1})*	n.d.[#]	n.d.	41 ± 6
EGME Specific surface area	*(m^2 g^{-1})*	72 ± 6	160 ± 23	333 ± 4
H_2O Specific surface area	*(m^2 g^{-1})*	131 ± 5	496 ± 12	442 ± 4
PZC		10.3 ± 0.3	10.1 ± 0.4	4.9 ± 0.7
Average particle size (pH 6.5)	*μm*	1.43 ± 0.2	0.92 ± 0.02	2.3 ± 0.1
ζ potential (pH 6.5)	*mV*	60 ± 2	33 ± 2	-13 ± 2
		After arsenate adsorption		
pH		6.76 ± 0.01	6.72 ± 0.03	6.51 ± 0.01
Average particle size	*μm*	0.86 ± 0.01	1.02 ± 0.08	1.19 ± 0.16
ζ potential	*mV*	-4.6 ± 0.2	-16.3 ± 0.4	-27.8 ± 0.4

[†] 40 days of aging time

[‡] 0 days of aging time

[§] Standard deviation

[#] Not detectable

Table 2. Langmuir parameters for the adsorption isotherms of arsenate on the three Al precipitation products, determination coefficient (r^2), standard error (SE) and significance (p) of the data fit to the Langmuir equation.

	Langmuir maximum adsorption (X_{MAX})		**Langmuir affinity constant (K_L)**	***r²***	***SE*** [#]	***p***
	mmol kg^{-1}	*μmol m^{-2}* [§]	*(mL μmol^{-1})*			
[†]**Crystalline Al hydroxide**	140 ± 2[#]	1.92 ± 0.04	198 ± 17	*0.999*	*2.1×10^{-5}*	*2.6×10^{-9}*
[‡]**Amorphous Al hydroxide**	291 ± 4	1.82 ± 0.04	11 573 ± 65	*0.999*	*1.4×10^{-6}*	*2.0×10^{-15}*
[†] **Al-tannate precipitate**	204 ± 5	0.61 ± 0.02	50 ± 25	*0.987*	*6.2 ×10^{-5}*	*6.6×10^{-7}*

[†] 40 days of aging time

[‡] 0 days of aging time

[§] Based on EGME (ethylene glycol monoethyl ether) specific surface area

[#] Standard error

Table 3. Arsenate adsorbed at 298 K by each Al precipitation product at different times, expressed as percentage of the arsenate initially added or as percentage of the arsenate adsorbed during the 24-h equilibration interval.

	% As(V) adsorbed				
	min				
	5	*30*	*60*	*720*	*1440*
	[†]Crystalline Al-hydroxide				
% added As	37 ± 0.2[§]	43 ± 0.1	45 ± 0.7	52 ± 0.4	54 ± 0.2
% As adsorbed after 24h	69 ± 0.2	79 ± 0.7	82 ± 0.3	96 ± 0.4	100
	[‡]Amorphous Al-hydroxide				
% added As	56 ± 0.1	72 ± 0.2	77 ± 0.1	94 ± 0.2	99 ± 0.1
% As adsorbed after 24h	57 ± 0.1	73 ± 0.1	78 ± 0.1	95 ± 0.2	100
	[†]Al-tannate precipitate				
% added As	6 ± 0.4	14 ± 0.4	16 ± 0.1	38 ± 0.1	46 ± 0.3
% As adsorbed after 24h	14 ± 0.9	30 ± 0.8	35 ± 0.3	83 ± 0.4	100

[†] 40 days of aging time

[‡] 0 days of aging time

[§] Standard deviation

Table 4. Values of determination coefficient (r^2), significance (p) and standard error (SE) for six different models fitted to the kinetics of arsenate adsorption on the three Al precipitation products at 298 K.

	Crystalline Al hydroxide[†]					
	Fast reaction (5-30 min)			*Slow reaction (40-720 min)*		
Model	r^2	*p*	*SE* [§]	r^2	*p*	*SE*
Zero order	0.975	6.7×10^{-3}	5.9×10^{-7}	0.957	3.8×10^{-3}	1.1×10^{-6}
First order	0.979	1.3×10^{-3}	6.8×10^{-7}	0.963	3.0×10^{-3}	1.8×10^{-6}
Second order	0.983	1.0×10^{-3}	6.4×10^{-7}	0.969	2.3×10^{-3}	1.7×10^{-6}
Elovich	0.979	1.3×10^{-3}	5.5×10^{-7}	0.969	2.3×10^{-3}	9.6×10^{-7}
Parabolic diffusion	0.995	2.0×10^{-4}	3.4×10^{-7}	0.989	5.0×10^{-7}	6.3×10^{-7}
Power law	0.984	8.0×10^{-4}	6.7×10^{-7}	0.974	1.8×10^{-3}	9.7×10^{-7}
	Amorphous Al hydroxide[‡]					
	Fast reaction (5-30 min)			*Slow reaction (40-720 min)*		
Model	r^2	*p*	*SE*	r^2	*p*	*SE*
Zero order	0.902	1.3×10^{-2}	3.5×10^{-6}	0.884	5.2×10^{-3}	4.7×10^{-6}
First order	0.939	6.6×10^{-3}	3.3×10^{-6}	0.975	2.4×10^{-4}	2.9×10^{-6}
Second order	0.967	2.5×10^{-3}	2.4×10^{-6}	0.991	3.3×10^{-5}	2.8×10^{-6}
Elovich	0.998	3.4×10^{-5}	4.8×10^{-7}	0.999	3.3×10^{-7}	4.3×10^{-7}
Parabolic diffusion	0.967	2.6×10^{-3}	2.9×10^{-7}	0.964	4.8×10^{-4}	9.6×10^{-7}
Power law	0.994	2.1×10^{-4}	5.9×10^{-7}	0.998	1.0×10^{-6}	4.9×10^{-7}
	Al-tannate precipitate[†]					
	Fast reaction (5-30 min)			*Slow reaction (40-720 min)*		
Model	r^2	*p*	*SE*	r^2	*p*	*SE*
Zero order	0.913	1.1×10^{-2}	1.5×10^{-6}	0.939	1.4×10^{-3}	4.2×10^{-6}
First order	0.920	9.8×10^{-3}	1.7×10^{-6}	0.957	7.1×10^{-4}	4.1×10^{-6}
Second order	0.927	8.6×10^{-3}	1.7×10^{-6}	0.972	3.0×10^{-4}	3.3×10^{-6}
Elovich	0.979	1.3×10^{-3}	7.2×10^{-7}	0.987	6.6×10^{-4}	2.0×10^{-6}
Parabolic diffusion	0.961	3.3×10^{-3}	9.6×10^{-7}	0.992	2.6×10^{-5}	6.1×10^{-7}
Power law	0.964	2.9×10^{-3}	8.8×10^{-7}	0.997	3.5×10^{-6}	2.3×10^{-6}

[†] 40 days of aging time

[‡] 0 days of aging time

[§] Standard error = $[\Sigma (A - A_m)]^2/(n - 2)]^{1/2}$, where A is the experimental value; A_m is the theoretical value based on modeling; n is the number of the data; the unit of SE is mol/L of As in solution

Table 5. The second-order rate constants for the fast and slow reactions of arsenate adsorption on the three Al precipitation products

	Second-order rate constants of the FAST reaction (5-30 min) **(M^{-1} h^{-1})**							**Second-order rate constants of the SLOW reaction** (40-720 min) **(M^{-1} h^{-1})**						
	Temperature (K)				*SE*†	*$LSD_{0.05}$*‡	*$LSD_{0.01}$*‡	Temperature (K)				*SE*	*$LSD_{0.05}$*	*$LSD_{0.01}$*
	288	*298*	*308*	*318*				*288*	*298*	*308*	*318*			
§**Crystalline Al hydroxide**	2.05×10^{3}	2.19×10^{3}	2.55×10^{3}	2.73×10^{3}	*4.21×10^{2}*	*9.72×10^{2}*	*1.41×10^{3}*	2.02×10^{2}	2.16×10^{2}	2.20×10^{2}	2.13×10^{2}	*2.29×10^{1}*	*6.71×10^{1}*	*9.76×10^{1}*
#**Amorphous Al hydroxide**	1.26×10^{4}	1.85×10^{4}	2.72×10^{4}	3.42×10^{4}	*1.16×10^{3}*	*2.68×10^{3}*	*3.90×10^{3}*	2.79×10^{3}	6.68×10^{3}	1.61×10^{4}	2.99×10^{4}	*1.32×10^{2}*	*3.05×10^{2}*	*4.43×10^{2}*
§**Al-tannate precipitate**	7.95×10^{2}	1.25×10^{3}	1.99×10^{3}	3.07×10^{3}	*1.73×10^{2}*	*4.00×10^{2}*	*5.83×10^{2}*	1.33×10^{2}	2.45×10^{2}	3.69×10^{2}	4.48×10^{2}	*2.92×10^{1}*	*6.76×10^{1}*	*9.83×10^{1}*
SE	*6.85×10^{2}*	*7.77×10^{2}*	*5.58×10^{2}*	*3.18×10^{2}*				*5.17×10^{1}*	*1.22×10^{2}*	*4.15×10^{1}*	*3.81×10^{1}*			
$LSD_{0.05}$	*1.58×10^{3}*	*1.80×10^{3}*	*1.29×10^{3}*	*7.36×10^{2}*				*1.19×10^{2}*	*2.83×10^{2}*	*9.58×10^{1}*	*8.81×10^{1}*			
$LSD_{0.01}$	*2.30×10^{3}*	*2.61×10^{3}*	*1.88×10^{3}*	*1.07×10^{3}*				*1.74×10^{2}*	*4.11×10^{2}*	*1.39×10^{2}*	*1.28×10^{2}*			

† Standard error

‡ Least significant difference at 95% ($LSD_{0.05}$) and 99% ($LSD_{0.01}$) levels

§ 40 days of aging time

0 days of aging time

Table 6: The activation energy (E_a) and pre-exponential factor (A) values for arsenate adsorption on the three Al precipitation products

	$\mathbf{E_a}$ *(kJ mol^{-1})*		**A** *(M^{-1} h^{-1})*	
	FAST reaction	*SLOW reaction*	*FAST reaction*	*SLOW reaction*
†**Crystalline Al hydroxide**	8 ± 2.6[§]	*NA* [#]	$6.5\times10^{4} \pm 5.8\times10^{3}$	*NA*
‡**Amorphous Al hydroxide**	26 ± 0.3	48 ± 1.3	$6.2\times10^{8} \pm 7.1\times10^{7}$	$1.5\times10^{12} \pm 7.2\times10^{11}$
†**Al-tannate precipitate**	34 ± 2.5	32 ± 0.4	$1.7\times10^{9} \pm 6.7\times10^{8}$	$1.1\times10^{8} \pm 1.5\times10^{7}$

† 40 days of aging time

‡ 0 days of aging time

§ Standard deviation

Not Applicable because the temperature dependence of the slow reaction of arsenate adsorption by the crystalline Al hydroxide was not statistically significant

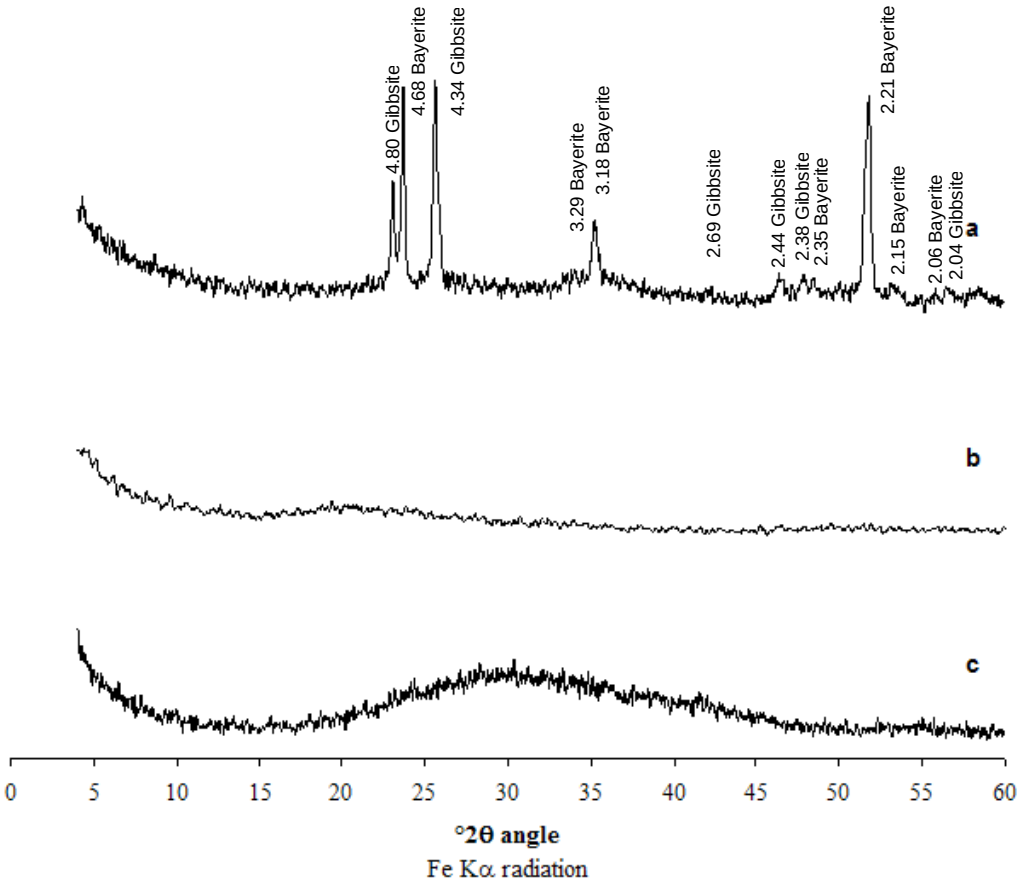

Figure 1. X-ray diffractograms of the three Al precipitates: (a) crystalline Al hydroxide, (b) pure amorphous Al hydroxide, and (c) Al-tannate precipitate formed at a tannate/Al molar ratio of 0.1.

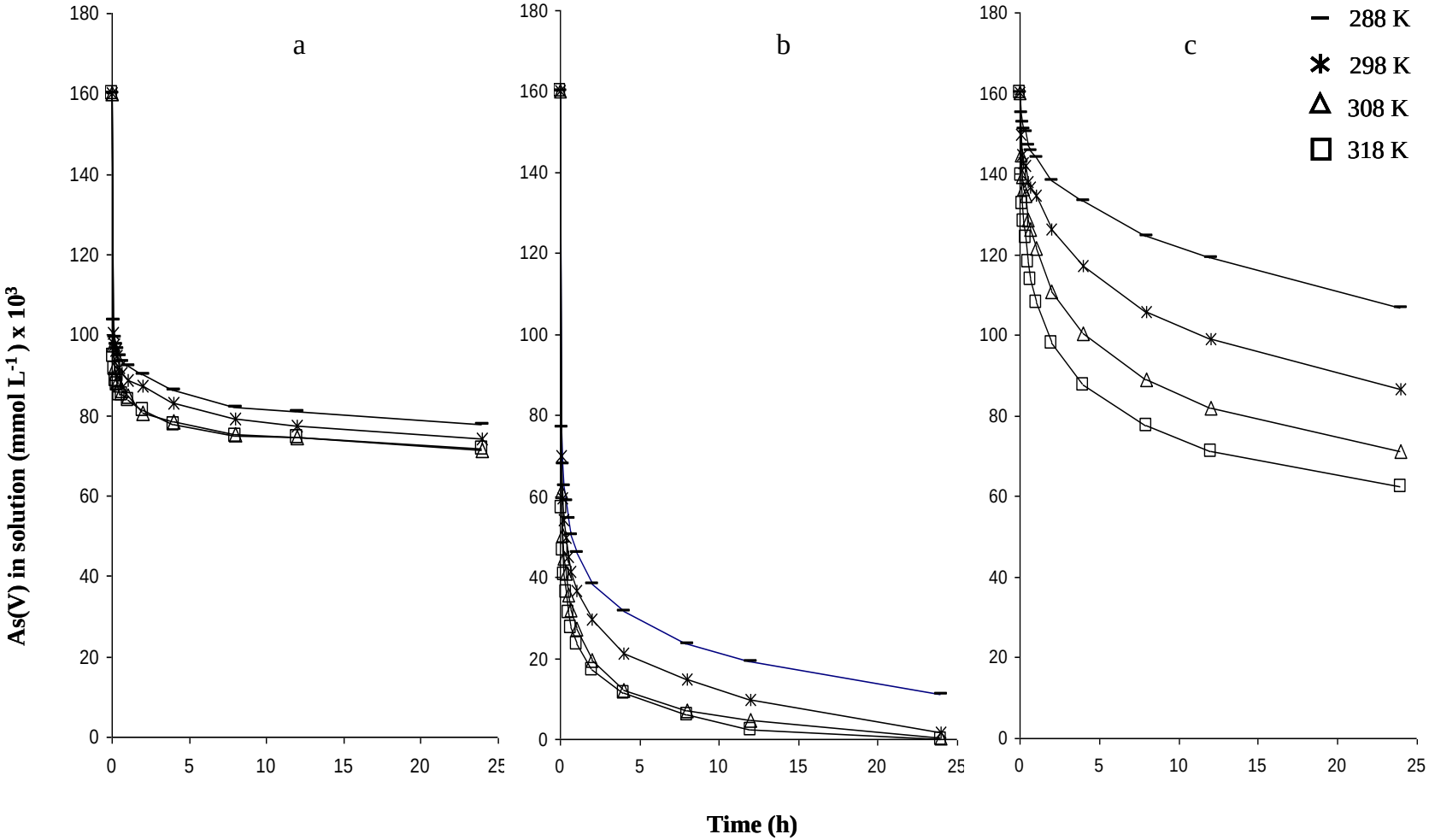

Figure 2. Time function of the concentration of arsenate in solution in the presence of: (a) crystalline Al hydroxide, (b) amorphous Al hydroxide, and (c) Al-tannate precipitate formed at a tannate/Al molar ratio of 0.1.

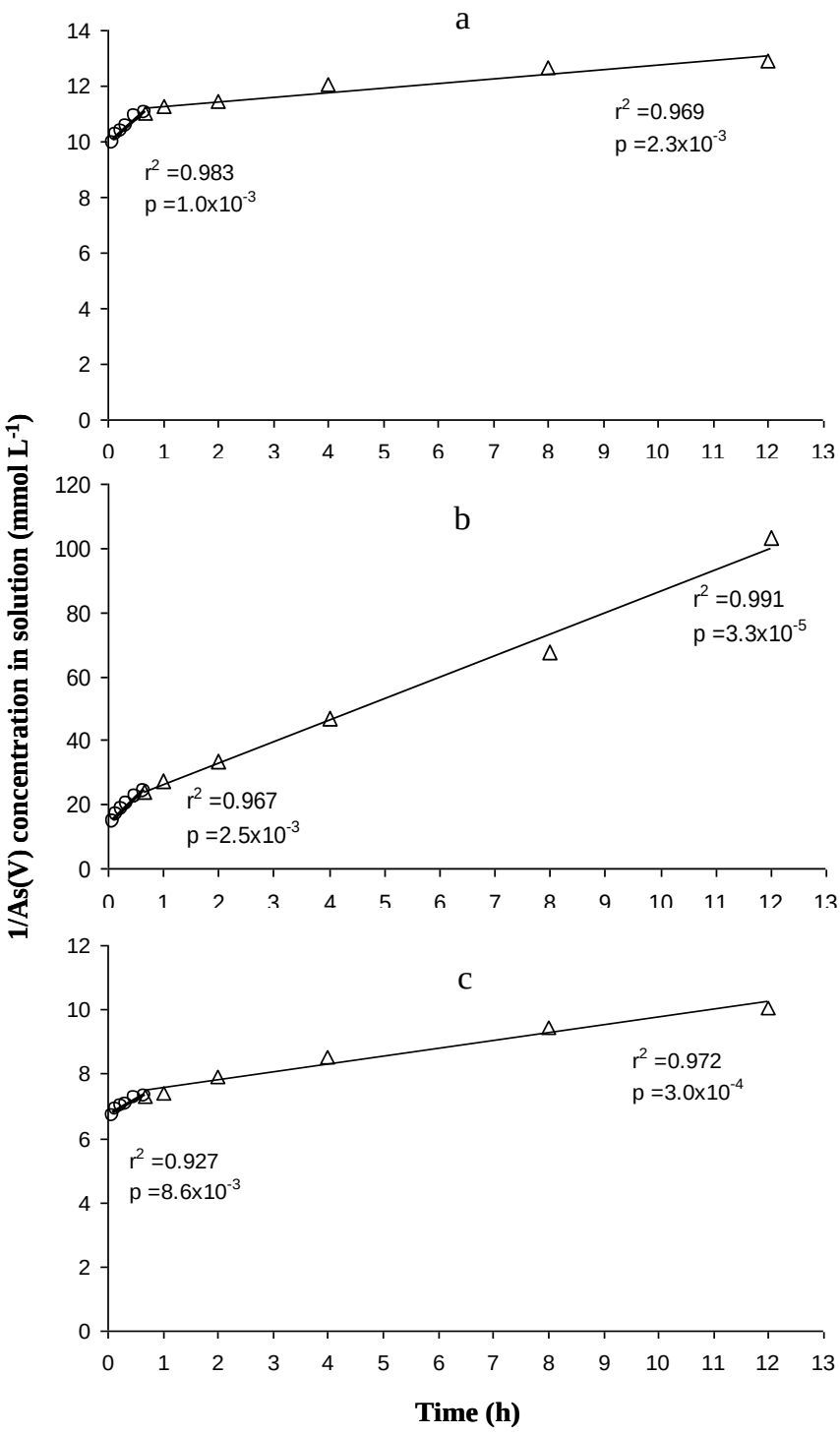

Figure 3. The second-order plots of arsenate adsorption at 298 K on: (a) crystalline Al hydroxide, (b) amorphous Al hydroxide, and (c) Al-tannate precipitation product formed at a tannate/Al molar ratio of 0.1.

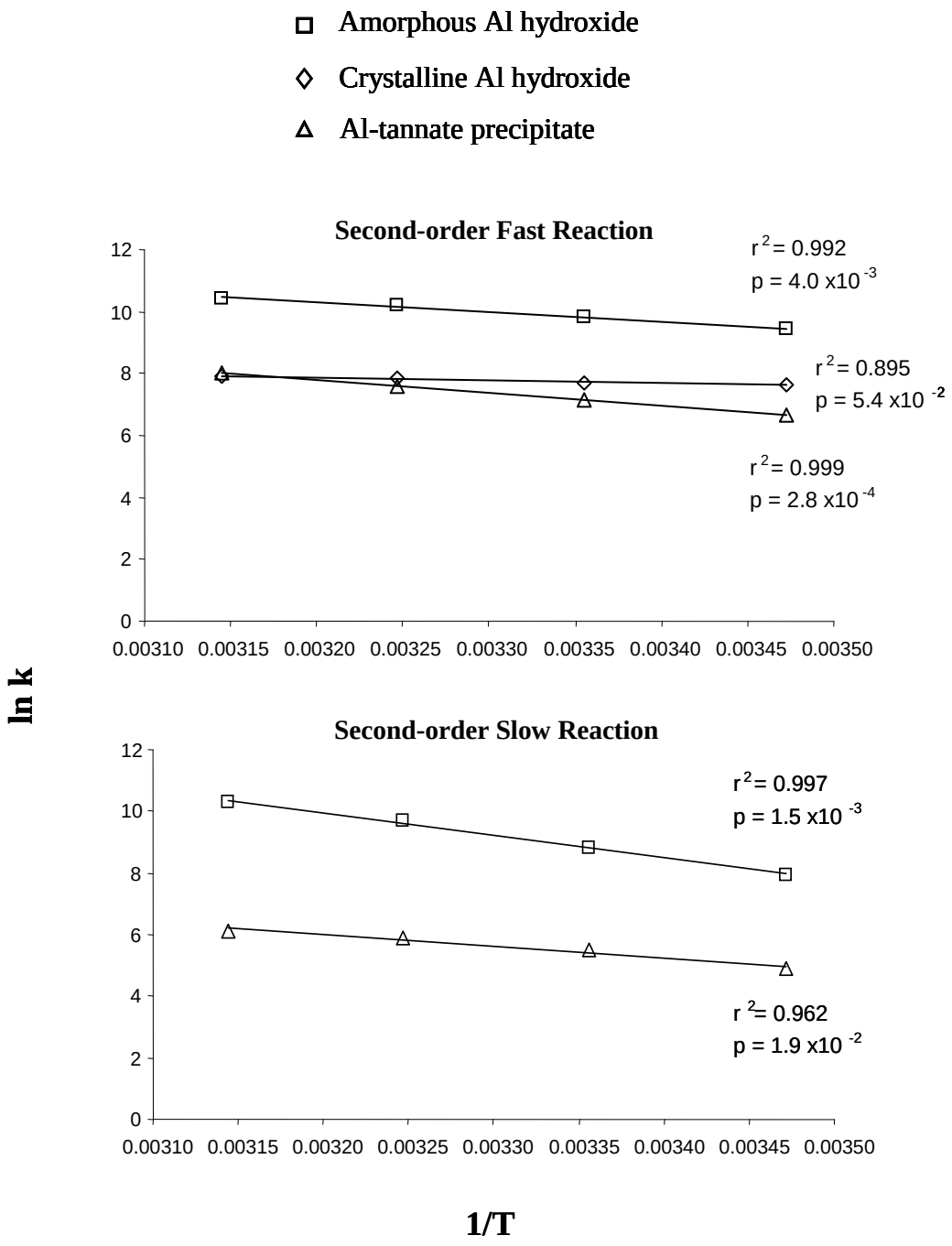

Figure 4. Arrhenius plots of arsenate adsorption kinetics on the three Al precipitation products; k (M^{-1} h^{-1}) is the second-order rate constant of arsenate adsorption and T (K) is the absolute temperature.